Automated virtual gauges for dimensional quality control

Rubén Usamentiaga*, Daniel F. Garcia,*, Francisco J. delaCalle

*Department of Computer Science and Engineering, University of Oviedo, Campus de Viesques
33204 Gijón, Asturias, Spain Tel.: +34-985-182626, Fax: +34-985-181986, Email: rusamentiaga@uniovi.es

***Abstract*—Dimensional quality control is a key issue in product manufacturing, particularly in long products such as rails or beams. To this end, international standards define precise methods to test if the dimensions are within the established tolerances, indicating whether they meet the required specification. The standards describe these methods using gauges that technicians can use to manually verify the dimensions of the product. In some cases, these methods provide different results from automated procedures, as they are based on different principles. To eliminate these discrepancies, this work proposes a novel automated method that emulates manual testing using virtual gauges. The proposed approach is based on an iterative procedure that aligns virtual gauges with the measured product shape, preventing one shape from penetrating another. This is achieved by assigning different weights to point correspondences according to their position. The result perfectly emulates the manual procedure, substituting the long and tedious manual procedure with a fast and robust automated alternative. Moreover, the proposed method can be applied to any dimensions with any type of gauge. Extensive tests with synthetic and manufactured rails corroborate the success of this approach.**[1]

***Index Terms*—Dimensional quality control, Long steel product, Inspection, Gauges, Conformance test**

I. Introduction

Automated quality inspection is a crucial step in industrial manufacturing for higher throughput and quality assurance [2]. Quality control has always been of interest, but in recent decades, the increased need for enhanced quality monitoring has led to a wide array of inexpensive sensors, capable of providing information about many different physical and internal properties of the inspected product. Examination of these properties ensures compliance with quality criteria before the products are used, guaranteeing the serviceability [3]. In addition, it prevents failures, which ensures safe long-term operation with important competitive advantages.

Dimensional quality control is a crucial step in automated quality inspection in many manufacturing industries [4]. The goal is to detect deviations between the manufactured product and its geometrical model. In dimensional quality control, the most common sensors to detect these possible deviations are the profilers [5]. These sensors project a laser line onto the inspected product and observe the projection with a camera. The projector-camera pair is calibrated, which makes a translation from image to real-world coordinates possible. This set of points that describes the surface of the product. The acquired set of points, or point cloud, can be compared with the geometrical model of the product. When the measured surface is not within the tolerances of the geometrical model of the inspected product, the manufactured product can be rejected.

Calibration, registration, reconstruction and measurement are the most important steps for dimensional quality control [6]. These areas are the source of numerous recent research works [7]–[9]. The most common approach is to first define a calibration procedure to translate from image to world coordinates. This calibration may also have to deal with multi-sensor configurations, where the coordinates from each sensor must be transformed into a common reference system. This step requires maximum accuracy in order to obtain a precise description of the surface of the inspected product. Registration is then used to align the set of points describing the surface of the product, the data, with the geometrical model. This step is usually performed using a variation of the least-squares best fit method. This optimization problem minimizes the distance between the data and the model iteratively. The goal of the reconstruction is the transformation of the aligned data into a geometrical description of the measured surface similar to the geometrical model, i.e., where the surface is described by a set of geometric primitives rather than points. This process can be carried out by fitting the points to the appropriate type of primitives, such as line segments or circular arcs based on the geometrical model description. Measurement is the final step for the detection of deviations between the manufactured product and the model. Measurement depends on the product, the dimension, and the standard used.

Dimensional quality control depends on the geometrical specification that describes the set of conditions that must be met by the manufactured product. For example, in the case of rails there are different standards, such as the EN-13674-1-2011 for Europe [10], the AREMA for America [11] or the GOST for the Russian Federation [12]. They describe the geometrical models of the rails, the dimensions and the maximum allowed tolerances for each dimension. When dimensional quality control is performed using automated procedures, a mathematical translation of the measured points on the surface of the inspected product is necessary in order to adapt to the measurement definition. For example, the EN-13674-1-2011 standard defines rail model 60E1 and the geometrical

[1]This is an extended version of the paper presented at the IEEE IAS Annual Meeting 2020 in Detroit [1]

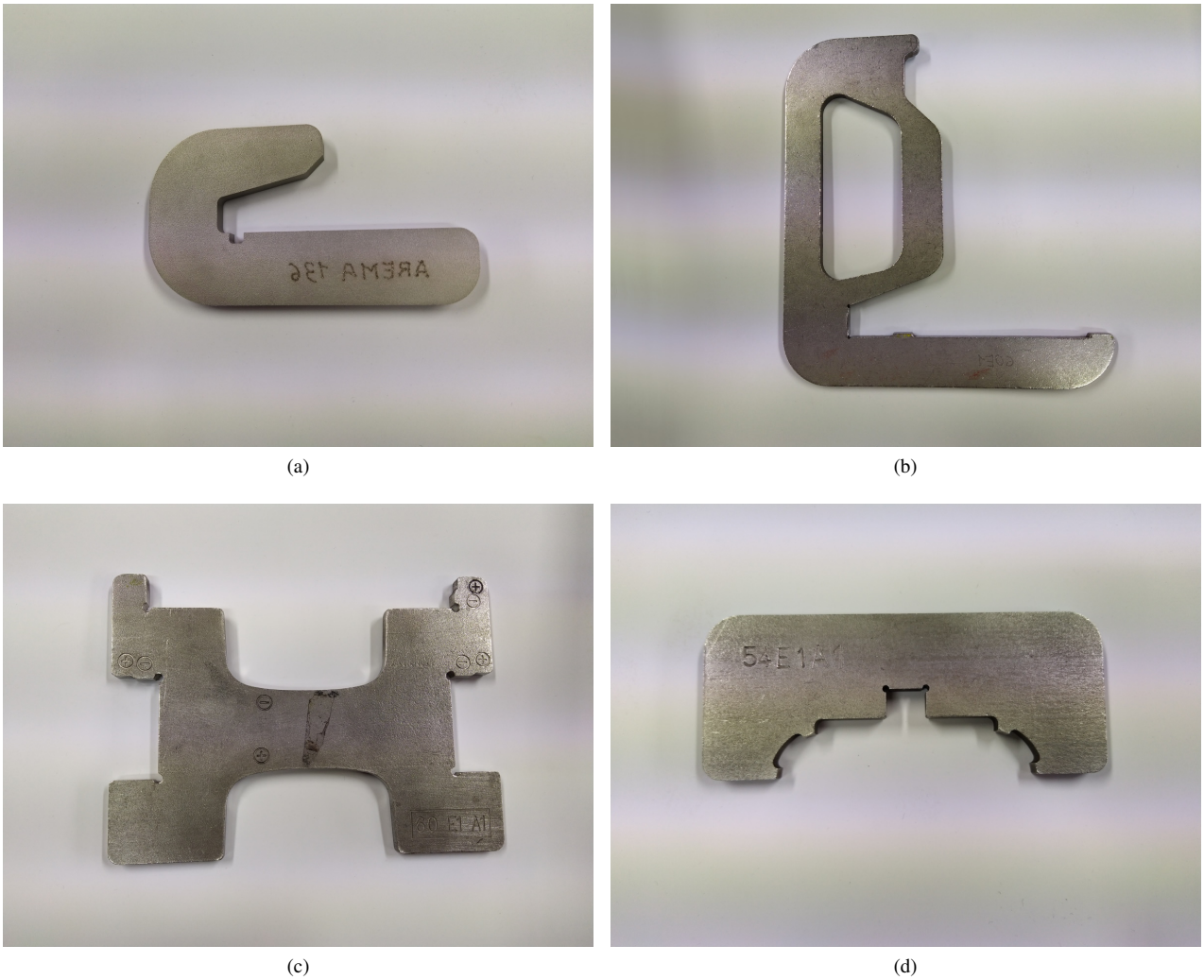

(a) (b)

(c) (d)

Fig. 1. Gauges used for dimensional quality control in rails. (a) Gauge used for testing the foot thickness. (b) Go gauge used for testing asymmetry. (c) Gauge used for testing head width. (d) Gauge used for testing head shape.

primitives of the head, the dimensions for the head width (72.01 mm) and the maximum tolerance for the head width ($\pm$ 0.5 mm). Automated measurement is usually performed by line-fitting the set of points that describe the surface of the line segments on both sides of the head, and then calculating the distance between the lines at a particular vertical position. However, depending on the particular algorithm used other tests can be performed. The distance from points to points, the distance from points to lines or planes, or the angle between lines are other common geometrical features calculated from the set of points describing the surface of the inspected product to verify that it meets the specification. Following this approach, all of the geometrical features of the inspected product are calculated from points measured on the surface.

The methods used to extract geometrical information from the inspected products in automated quality inspection cannot be emulated in manual quality control. Technicians cannot measure the positions of points on a surface manually, so a different procedure is required. In the case of mass-produced products, technicians perform dimensional quality control with the help of gauges, which can be used to quickly validate whether the dimensions of the product are within the allowable tolerances. These gauges, including the commonly referred to as go/no-go gauges, are mechanical artifacts used for checking a product [13]. They are not used to measure the size of the product, but only to verify that the dimensions of the product are within the specified limits. The go gauge is used to check for the minimum valid condition and the no-go gauge for the maximum. Figure 1 shows some examples of gauges used for rail inspection. The gauges are placed on the rail to verify the dimensions, as can be seen in Figure 2.

In most manufactured products the same results are obtained when using gauges, in manual quality control, as when using a sensor to acquire information about points on the surface of the product and then performing automated measurement, in automated quality control. One difference between the two approaches is that automated quality control also provides a quantitative measurement of each particular dimension. There

(a) (b)

Fig. 2. Positioning the gauge on the rail for manual quality control of the asymmetry after manufacturing.

are also cases where the conformance test used to validate the product using a manual or an automated procedure provides different results. This difference lies in the way the gauges are handled. For example, the asymmetry gauge in Figure 1b is used to test the asymmetry of the rail. For this dimension, there are two types of gauges: the go and the no-go gauge. With the go gauge, the gauge must touch the foot of the rail but not the head, and vice versa with the no-go. The free space in the area where the gauge must not touch the rail represents the tolerance. The operation with these two gauges is illustrated in Figure 3. When the technician places the gauge on the rail, the gauge is also placed under the foot of the rail, touching the surface of this area. Thus, a small deviation in the foot can affect the conformance test of the asymmetry. Similarly, the gauge used to validate the head width in Figure 1c is also affected by the shape of the head. These issues affect the result of the conformance test, leading to positive validations when a particular dimension is measured using automated procedures and negative validations when they are performed manually. Moreover, the conformance tests described in the manufacturing standards only specify manual testing using gauges. Consequently, there are cases where automated procedures used during manufacturing validate the product, but the client that receives the product files a complaint because it does not meet the specifications with manual testing using the gauges described in the relevant standard. This can be considered a failure of the automated validation procedure.

This work proposes a novel solution to eliminate the differences between automated and manual validation in dimensional quality control: the design of an efficient new automated method based on virtual gauges to emulate manual testing. This new approach to quality control preserves the higher throughput and quality assurance of automated methods, but also ensures compliance with manual testing using gauges established in international standards. Using virtual environments to emulate manual procedures has been applied to other fields. However, the proposed approach is different as it meets the extreme accuracy requirement in testing where tolerances are under 0.5 mm. For example, virtual surgery employs a similar approach for testing the interpenetration between a virtual deformable organ and a rigid tool controlled by the user [14]. However, they approximate the objects using bounding boxes in order to achieve high performance, which degrades accuracy. On the contrary, this work proposes a method that is fast, but also accurate and robust. The proposed approach to perform physical emulation is based on four steps. First, the alignment of the measured data that contains information about the surface of the manufactured product with the model. Then, virtual gauges are created based on the standards specification and coarsely aligned with the data. The next step is a fine alignment between the data and the virtual gauges introducing weighted coefficients to ensure the same tangential alignment a technician performs manually using physical gauges. Finally, a conformance test validates the product. The result is a fast and robust procedure that can be easily integrated into automated quality control, preventing potential discrepancies between testing approaches. The proposed approach is validated with synthetic and real data.

This paper is organized as follows: Section II presents the proposed approach to use virtual gauges for dimensional control quality; Section III discusses the results obtained, and finally, Section IV reports conclusions.

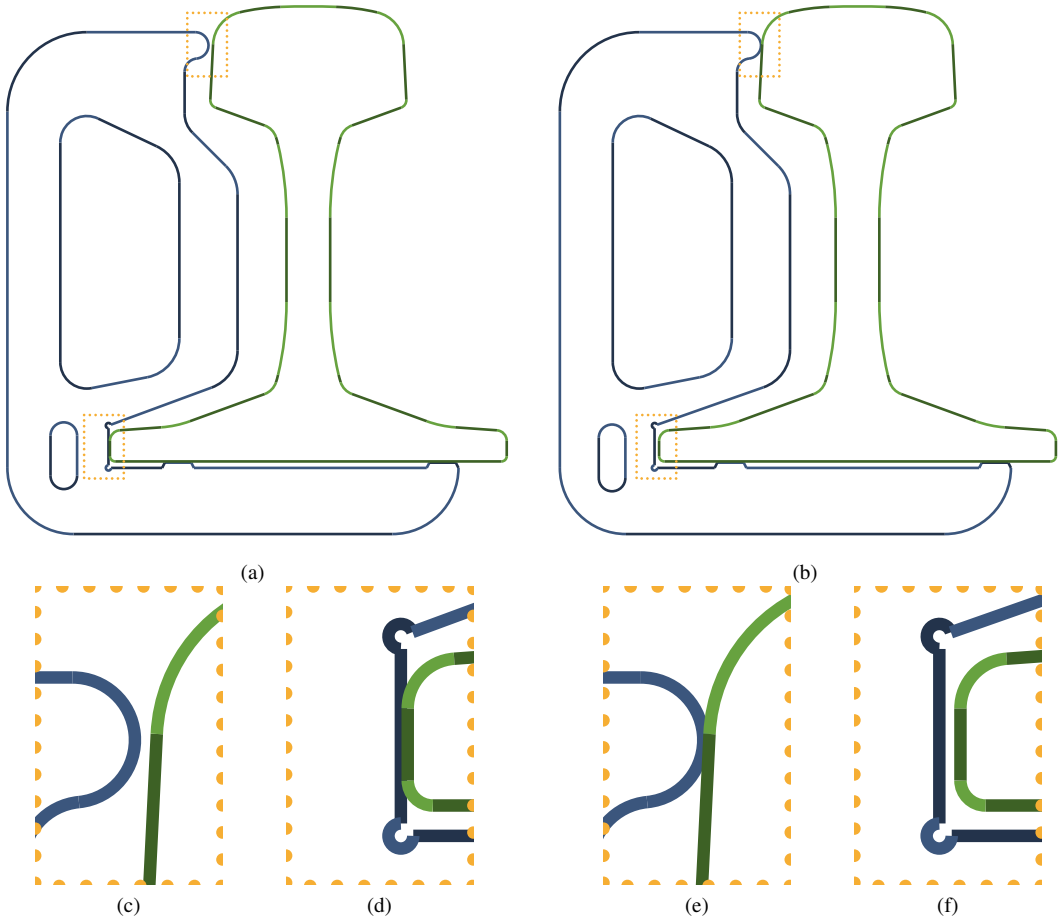

Fig. 3. Positioning the gauge on the rail for manual quality control of the asymmetry. (a) Go gauge: the gauge collides with the rail on the foot but not the head. (b) No-go gauge: the gauge collides with the rail on the head but not on the foot. (c), (d) Separation on the head and on the foot for go gauge. (e), (f) Separation on the head and on the foot for no-go gauge. The separation represents the tolerance of the dimension.

II. Proposed approach

The proposed approach is divided into four steps, as can be seen in Figure 4. The goal is to emulate manual testing using virtual gauges on the measured surface of the manufactured product.

A. Alignment of the data with the model

The first step is the acquisition of 3D information about the shape of the product and the registration or alignment of the measured data with the geometrical model. Previous research works deal with these problems extensively [6], [15]. The most common approach is to use multiple 3D sensors that provide different views of the product that are combined into a single reference system. The result is a single profile with information about the shape of a section of the manufactured product. Registration is then applied to the acquired data. This procedure aligns the data with the geometrical model of the manufactured product. Reconstruction and measurement are performed next. The approach proposed in this work starts with the registration of the data and the model.

The goal of this step is the registration of the profile with the geometric model of the product. The product moves during manufacturing, and the registration translates and rotates the acquired profile according to the model. This procedure is generally applied in two consecutive phases: coarse registration and fine registration. The first phase is based on the centroid and principal component analysis. The second phase is based on the ICP (Iterative Closest Point) algorithm [16]. This algorithm approximates the profile and the model iteratively by estimating point-model correspondences and rigid body transformations.

Figure 5a shows the model of a rail and a profile measured by a 3D sensor. In this case, the profile has been synthetically generated from the model, and then translated. Thus, the profile is a perfect representation of the expected model. The alignment of the data with the model gives Figure 5b, where the profile is rigidly transformed to match the position of the model. As the profile is a perfect discretion of the model, it accurately overlaps with the shape.

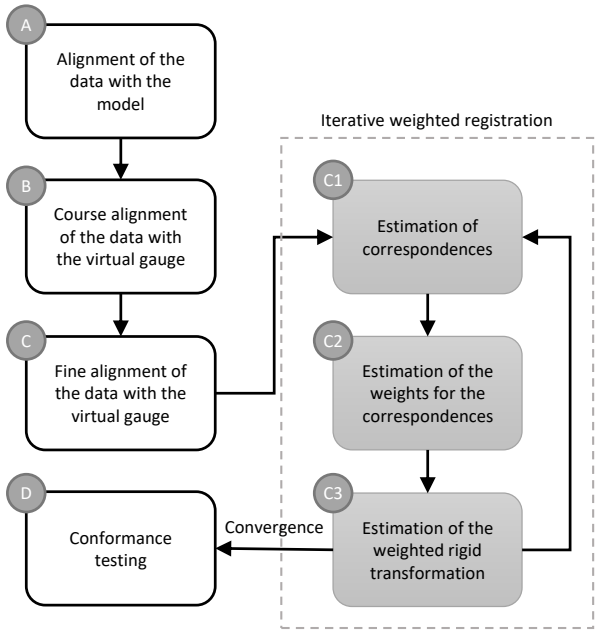

Fig. 4. Flowchart of the proposed approach.

B. Course alignment of the data with the virtual gauge

The alignment of the data with the model provides a good approximation of the position of the profile. Therefore, the initial position of the virtual gauge can be calculated considering the position of the data. This represents a coarse alignment, i.e., a coarse approximation of the virtual gauge, as the shape of the data can change depending on the model and the possible manufacturing issues. However, it is a good starting point for the fine alignment, which can only obtain a globally optimal solution when the data is close to the model.

Figure 5c show the initial coarse alignment of the data with the virtual gauge. As can be seen, it is only a rough approximation in which the shapes of profile and gauge do not touch.

C. Fine alignment of the data with the virtual gauge

The fine alignment of the data with the virtual gauge is the most important step of this approach. This alignment must emulate the physical process of placing the gauge on the manufactured product. Therefore, the shape of the virtual gauge cannot penetrate the data that represents the shape of the profile. This makes the problem very different from shape registration, in which the global optimum is reached when the least square error is minimized. In this case, the least square error must be minimized with a major restriction: shape penetration is not allowed. The approach is a variation of the ICP algorithm consisting in an iterative rigid transformation of the data based on the estimation of weighted correspondences with the model.

The procedure is illustrated using the model and the data in Figure 6 as an example. The beginning of the problem can be seen in Figure 6a, including the gauge (represented at the bottom of the figure) and the data (represented at the top of the figure with a sinusoidal base).

1) Estimation of correspondences: First, correspondences are estimated between every point in the data and the closest point in the model. This mathematical problem is solved using an analytical approach by considering the geometric primitives of the virtual gauges. This approach is not only faster, but also much more accurate.

Figure 6b shows arrows with the correspondences between some of the points of the data with the model of the virtual gauge.

2) Estimation of the weights for the correspondences: Not all correspondences have the same weight for the estimation of the rigid transformation. In the alignment between the data and the model of the virtual gauge, no penetration between the shapes is allowed. Therefore, the points in the data located inside the shape of the virtual gauge have more weight than those outside. Changing the weight of some points gives more importance to some correspondences than to others. Thus, the optimization problem that tries to find the optimal alignment of the data and the model will use the weights to achieve the desired result avoiding shape penetration. The approach in this work is to give a weight of 1 to those correspondences where the point of the data is outside the virtual gauge. If the point is inside the virtual gauge, the weight of the correspondence is equal to the number of points in the data. This way, a single point inside the virtual gauge will have more combined weight than the rest of points, even if they are all outside. The goal is that the iterative procedure will move the data to avoid shape penetration considering the assigned weights.

Whether a point in the data is inside the virtual gauge can be calculated using the normal vector of the closest geometric primitive of the point in the data, and the vector from the point to the closest point in the geometric primitive. When the dot product between these two vectors is positive, it means the point is inside the shape of the gauge. It is negative otherwise. This procedure, which works with linear or circular primitives, assumes that the geometrical primitives are ordered.

In Figure 6b all the points in the data are outside the virtual gauge. Thus, they all have the same weight: 1.

3) Estimation of the weighted rigid transformation: Once the weights of the correspondences are calculated, the rigid transformation between the correspondences must be calculated. A rigid transformation, also called Euclidean transformation, is a geometric transformation that preserves the Euclidean distance. This type of geometric transformation is composed of translations and rotations. Reflections can also be part of a rigid transformation, but they are generally excluded. A rigid transformation is commonly used to align two sets of points [17]. This approach can also be used to align a point cloud measured from an object to a CAD model of this object by using an iterative procedure [18].

A rigid transformation can be defined using (1), where the combination of R (rotation) and t (translation) provides a mapping between point set $\mathcal{P}$ and point set $\mathcal{Q}$. These point

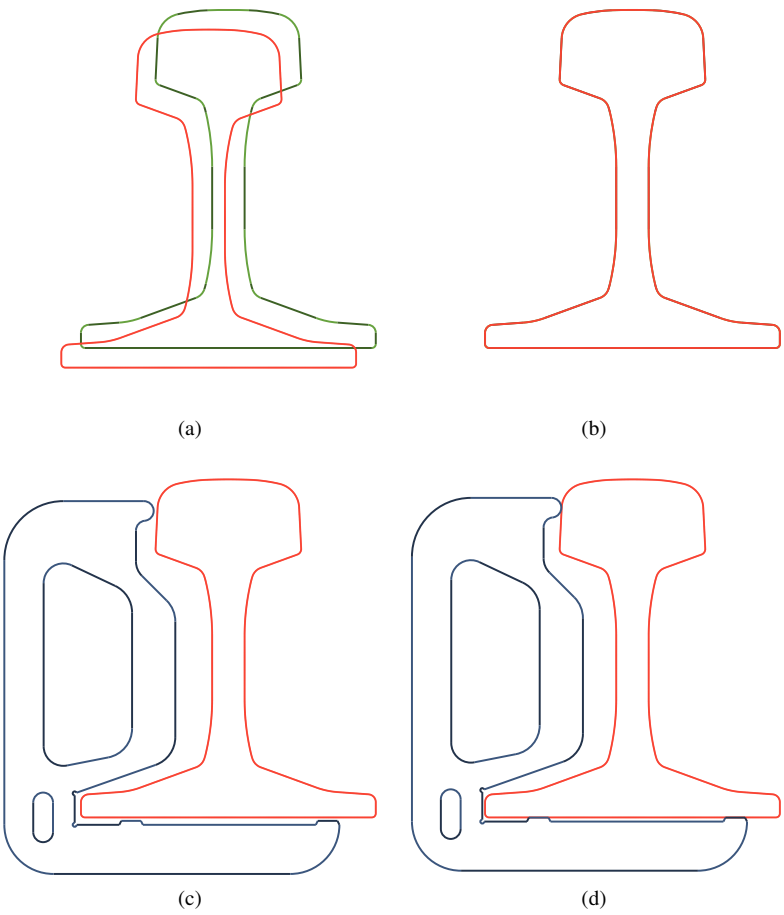

Fig. 5. Processing steps of the proposed approach. (a) A profile and model for a particular rail. (b) Alignment of the data with the model. (c) Course alignment of the data with the virtual gauge. (d) Fine alignment of the data with the virtual gauges.

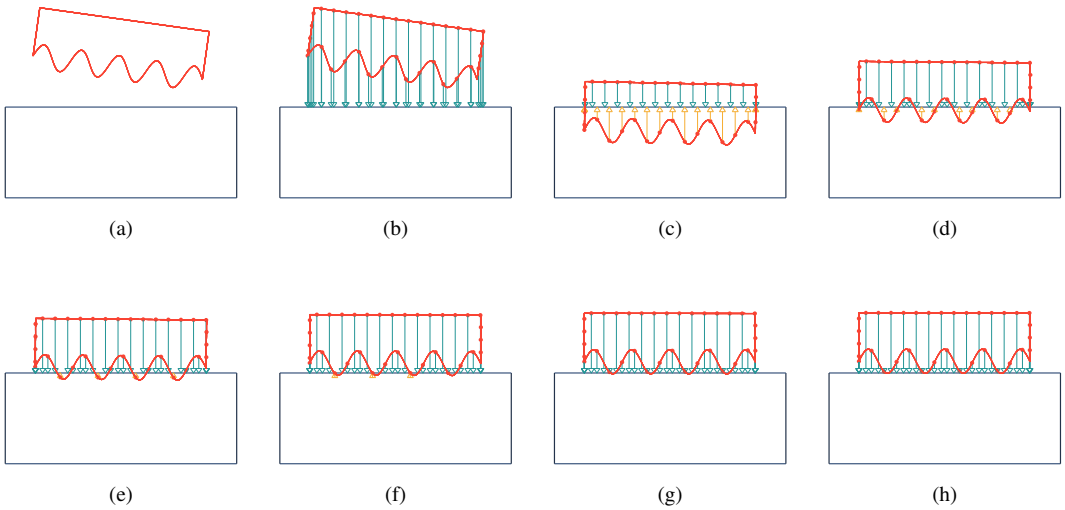

Fig. 6. Example of fine alignment of the data with the virtual gauge. (a) Beginning of the problem: gauge on bottom of the figure and data on top of the figure with a sinusoidal side. (b) Initial estimation of correspondences. (c)-(h) Result of iterations from 1 to 6 and new estimation of correspondences.

sets contain n points defined in $\mathbb{R}^d$, $\mathcal{P} = \{p_1, p_2, \ldots, p_n\}$, and $\mathcal{Q} = \{q_1, q_2, \ldots, q_n\}$. In 2D, a point, p_i, is defined using 2 coordinates $p_i = (p_{ix}, p_{iy})^T$, R is a 2×2 rotation matrix and t is 2D translation vector.

$$\mathcal{Q} = \mathcal{P}R + t \tag{1}$$

The estimation of the rigid transformation requires solving (1) for the optimal rotation and translation (R and t) that maps $\mathcal{P}$ onto $\mathcal{Q}$. This requires minimizing the square difference, E, given by (2). The estimation of the rigid transformation can be affected by a set of weights, W, that can quantify the certainty about some point correspondences.

$$E = \sum_{i=1}^{n} W \left| \mathcal{P}R + t - \mathcal{Q} \right|^2 \tag{2}$$

The optimal translation can be calculated by taking the derivative of E and searching for the roots using (3).

$$0 = \frac{\partial E}{\partial t} = \sum_{i=1}^{n} 2W \left| \mathcal{P}R + t - \mathcal{Q} \right| \tag{3}$$

Equations (4), (5) and (6) are obtained by rearranging the terms of (3).

$$-2t \sum_{i=1}^{n} W = 2R \sum_{i=1}^{n} W\mathcal{P} - 2 \sum_{i=1}^{n} W\mathcal{Q} \tag{4}$$

$$t = \frac{2R \sum\limits_{i=1}^{n} W\mathcal{P}}{-2 \sum\limits_{i=1}^{n} W} - \frac{2 \sum\limits_{i=1}^{n} W\mathcal{Q}}{-2 \sum\limits_{i=1}^{n} W} \tag{5}$$

$$t = \frac{\sum\limits_{i=1}^{n} W\mathcal{Q}}{\sum\limits_{i=1}^{n} W} - R \frac{\sum\limits_{i=1}^{n} W\mathcal{P}}{\sum\limits_{i=1}^{n} W} \tag{6}$$

The optimal translation, t, can then be calculated using (7), where $\mathcal{P}^c$ and $\mathcal{Q}^c$ represent the weighted centroid of $\mathcal{P}$ and $\mathcal{Q}$ in (8).

$$t = \mathcal{Q}^c - R\mathcal{P}^c \tag{7}$$

$$\mathcal{Q}^c = \frac{\sum\limits_{i=1}^{n} W\mathcal{Q}}{\sum\limits_{i=1}^{n} W}, \; \mathcal{P}^c = \frac{\sum\limits_{i=1}^{n} W\mathcal{P}}{\sum\limits_{i=1}^{n} W} \tag{8}$$

Substituting the optimal t in (2) and rearranging terms gives (9). Thus, the problem requires the calculation of the optimal rotation matrix that minimizes the root mean squared deviation between the two paired sets of points: $\mathcal{P}^z = \mathcal{P} - \mathcal{P}^c$, and $\mathcal{Q}^z = \mathcal{Q} - \mathcal{Q}^c$. These are two sets of points centered at the weighted centroids of the original points.

$$E = \sum_{i=1}^{n} W \left| R(\mathcal{P} - \mathcal{P}^c) - (\mathcal{Q} - \mathcal{Q}^c) \right|^2 \tag{9}$$

The general approach for solving (9) involves calculating the cross-dispersion matrix [17].

The standard method for estimating R for 3D points is to calculate the cross-dispersion matrix, which is defined as (10). The cross-dispersion matrix is then decomposed using SVD.

$$C = \frac{1}{n} \sum_{i=1}^{n} W\mathcal{P}^z \mathcal{Q}^{zT} \tag{10}$$

In 2D, the procedure can be greatly simplified, as the equation depends on a single variable: the rotation angle. Therefore, the derivative with respect to this angle can be calculated. The result is (11). The optimal value of the angle can be used to calculate R and t, i.e., the rigid transformation that maps one set of points onto the other.

$$\theta = \tan^{-1} \left(\frac{\sum\limits_{i=1}^{n} (W_i p_{ix}^z q_{iy}^z - W_i p_{iy}^z q_{ix}^z)}{\sum\limits_{i=1}^{n} (W_i p_{ix}^z q_{ix}^z + W_i p_{iy}^z q_{iy}^z)} \right) \tag{11}$$

The described procedure can be used to estimate the weighted rigid transformation from the correspondences in Figure 6b. Applying the estimated transformation to the initial data results in the transformed data in Figure 6c.

4) Iterative weighted registration: The registration repeats the previous steps: estimation of correspondences, calculation of weights, and estimation and application of the weighted transform. Figure 6c shows the results of the first iteration. Then, new correspondences are estimated again. In this case, some points are located inside the virtual gauge and others outside (they are shown with different colors in the figure). Thus, their weight will be different according to this approach: inside points will always have increased weight. The result of the second iteration is shown in Figure 6d. As can be seen, the data is displaced upwards because the points inside the gauge pull the data in this direction. The procedure is repeated until convergence, which is detected when the data does not move between iterations. The final result can be seen in Figure 6h, which shows the alignment of the data and the virtual gauge without shape penetration. This emulates the physical process that a technician follows during manual quality control.

The iterative weighted registration applied to the data in Figure 5c results in the transformed data in Figure 5d. Thus, the result is the same as the technician would get when using the physical gauge.

D. Conformance testing

The last step of the proposed approach is conformance testing. Go/no-go gauges test the position where the gauge and the profile touch, as can be seen in Figure 5d. Other gauges use a measuring rod with a specific thickness to verify the separation between the gauge and the manufactured product. Therefore, slightly different procedures are required for conformance testing depending on the particular type of gauge used. However, once a virtual gauge is placed on the profile, the specific conformance testing procedure can be easily adapted.

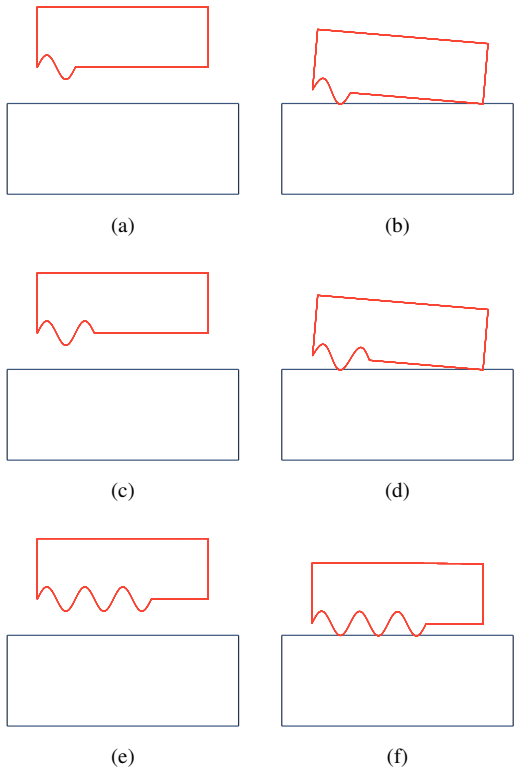

Fig. 7. Example of fine alignment of different shapes with the virtual gauge. (a) Shape with a one-period sine. (b) Alignment results with a one-period sine. (c) Shape with a two-period sine. (d) Alignment results with a two-period sine. (e) Shape with a three-period sine. (f) Alignment results with a three-period sine.

III. Results and Discussion

A. Synthetic tests

Synthetic shapes are aligned with virtual gauges for testing the procedure. Variations of the example presented in Figure 6 are tested to verify the ability of the procedure to emulate what a technician would do with different shapes.

Tests with synthetic shapes can be seen in Figure 7. Three different shapes are used with one, two and three-period sine curves on the bottom. This gives rise to a unique problem when performing the alignment. The procedure must emulate what a technician does, which includes gravity. Thus, in the first and second cases the alignment with the virtual gauge rotates the shape. This is what happens when a technician places the product on the gauge (or the gauge on the product). The proposed approach emulates this behavior perfectly, giving an accurate registration without shape penetration. The result in the third case is different as the curvature on the bottom of the shape is longer. Thus, it is more natural to place to shape without the rotation, as it would naturally maintain the equilibrium. The alignment procedure is emulating this behavior without complicated physical models: only the weights control the final result, producing an easy to interpret method. The iterative alignment produces the desired result by simply controlling the weights of the correspondences, both outside and inside.

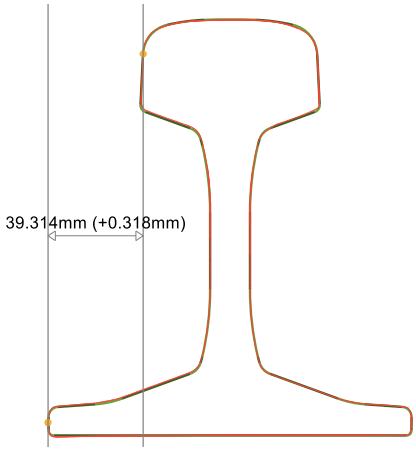

Fig. 8. Standard dimensional quality control using an automated procedure. The asymmetry of the rail is within the maximum tolerance.

The proposed approach produces results in accordance with those of a manual testing procedure. Thus, it could replace the manual procedure, giving the same result, with all the advantages of a robust and automated quality inspection.

B. Tests with rails

This is designed to eliminate the discrepancies between automated dimensional quality control and manual testing using gauges. These discrepancies can be analyzed using a rail and the asymmetry dimension.

The value of the asymmetry dimension for rail 60E1 is 39.0 mm with a maximum tolerance of ± 1.2 mm according to standard EN-1374 XB. A profile acquired from this rail and the asymmetry gauges can be seen in Figure 3. The asymmetry is calculated as the horizontal difference between the furthest point on the left of the fitted primitive of the left foot, and the top point of the fitted primitive of the left segment in the head. As can be seen, in this case the asymmetry is 39.314 mm. Thus, there is a deviation of +0.318 mm from the standard, well under the 1.2 mm maximum tolerance. Consequently, this rail will pass the conformance test.

The same profile can be tested using the proposed approach. The steps are shown in Figure 9. Figure 9a shows the initial profile acquired from the rail that provides information about the shape. Due to vibrations, the profile is not aligned with the geometrical model of the rail. Figure 9b shows the results after the profile is aligned with the model. This provides a good approximation of the location of the profile. The next step, shown in Figure 9c, places the virtual gauge in the vicinity of the rail profile. This coarse alignment is the initial position required for the fine alignment of the profile and the virtual gauge. The result of the final alignment can be seen in Figure 9d. The result is similar to what would have been obtained using a manual procedure. Thus, the proposed approach emulates manual quality control. It can be seen how the profile touches the virtual gauge both on the head and on the foot. The enlarged figures show the contact in both areas of the rail. This result indicates a failed conformance test, as this

gauge should not touch the foot. However, this contradicts the previous result using measurement in the standard automated procedure, which indicates that the asymmetry is within the standard tolerance.

In order to evaluate the proposed approach and to analyze the discrepancy with the standard automated procedure, the previous rail was manually tested and failed the conformance test. The result of this test corroborates the results in this work. The proposed work emulates the manual procedure, providing the same result. The reasons for the discrepancy lies in the shape of the measured profile. As can be seen in Figure 9b, the profile does not follow the model of the rail accurately. Slight deviations on the bottom of the left foot and of the underside of the head can be seen. These deviations affect how the gauge is placed on the rail, particularly under the foot. The deviations finally produce major discrepancies between the manual and the standard automated procedures.

Similar tests were repeated for a number of rails. The classification for some of these rails using the standard automated procedure and the manual were different. However, in all cases, the proposed approach resulted in a similar classification pass/fail to the manual approach. The results corroborate the success of the proposed procedure to accurately emulate manual quality testing. Therefore, what once was a manual procedure can now be applied to new automated procedures with the same results, greatly reducing the cost of the inspection.

Using virtual gauges for dimensional control quality could be applied to emulate any manual procedure, including testing with any gauge or dimension. Figure 10 shows the results of applying the proposed procedure to a different gauge: the head gauge. This type of gauge is used to test the shape of the head of a rail. Unlike asymmetry gauges, a single gauge is placed on the head to test if there is a gap between the gauge and the rail. If the gap is large enough to introduce a determined measuring rod, it indicates that the shape of the rail is not within the maximum allowed tolerance, failing the test.

The steps in Figure 10 are similar to those in Figure 9 with a different gauge. The difference can only be found after the virtual gauge is aligned with the rail. In the case of the asymmetry gauge, the conformance test must verify if there is any contact between the foot and the rail. However, in the case of the head gauge, the maximum distance between the measured profile and the gauge must be calculated. As can be seen in the enlarged views of the head in Figures 10e and 10f, this profile shows a fabrication defect: there is a lack of material. In order to assess this deviation from the model quantitatively, a procedure calculates the maximum distance from an region of the profile to the virtual gauge. This procedure emulates introducing the measuring rod to verify the gap between profile and gauge. In this case, the difference is 0.766 mm above the established tolerance. Different tests were performed to validate the proposed procedure using this type of virtual gauge. The results again corroborated the success of the proposed method, showing an average error of less than 0.1 mm in all cases. Thus, this manual test could be also substituted for the new automated procedure proposed in this work.

IV. Conclusions

Because the standards' definition of a valid product, dimensional quality control is usually performed using gauges and manual procedures. Automated procedures using a variety of sensors are rapidly replacing these manual approaches. However, there are cases where the manual and the standard automated approach do not produce the same results. This creates ambiguity when deciding whether a product meets the required specifications.

This work proposes an automated procedure to emulate manual testing in dimensional quality control. The proposal is based on 3D sensors that measure the shape of the product and virtual gauges that emulate the gauges used in manual testing. This work proposes an iterative application of the weighted rigid transform to align the virtual gauge with the inspected product preventing one shape from penetrating another, obtaining the same result a technician would get when placing the gauge during manual testing. Therefore, this novel automated procedure can substitute manual testing. Not only does this method eliminate the cost of testing the products manually, it also eliminates the need to make precise gauges for each single product model and dimension. In the case of rails, this represents a major investment.

Tests using synthetic models and real rails indicate the proposed method is a true substitute for the manual procedure using gauges. Improved automated quality control can add this new approach to provide more robust and complete tests for the manufactured products with no additional costs.

Acknowledgements

This work has been partially funded by the project RTI2018-094849-B-I00 of the Spanish National Plan for Research, Development and Innovation.

References

[1] R. Usamentiaga, D. Garcia, and F. delaCalle, "Automated virtual gauges for dimensional quality control," in *2020 IEEE Industry Applications Society Conference*, vol. 1. IEEE, 2020, pp. 1–8.

[2] S. Robinson, *Automated inspection and quality assurance*. Routledge, 2017.

[3] R. Usamentiaga, Y. Mokhtari, C. Ibarra-Castanedo, M. Klein, M. Genest, and X. Maldague, "Automated dynamic inspection using active infrared thermography," *IEEE Transactions on Industrial Informatics*, vol. 14, no. 12, pp. 5648–5657, 2018.

[4] M. Trapp and F. Chen, *Automotive buzz, squeak and rattle: mechanisms, analysis, evaluation and prevention*. Elsevier, 2011.

[5] G. Petrie and C. K. Toth, "Introduction to laser ranging, profiling, and scanning," in *Topographic laser ranging and scanning*. CRC Press, 2018, pp. 1–28.

[6] R. Usamentiaga, D. F. Garcia, and F. J. delaCalle Herrero, "Geometric reconstruction and measurement of long steel products using 3-d sensors in real time," *IEEE Transactions on Industry Applications*, vol. 55, no. 5, pp. 5476–5486, 2019.

[7] H. Liu, Y. Li, Z. Ma, and C. Wang, "Recognition and calibration of rail profile under affine-distortion-based point set mapping," *IEEE Transactions on Instrumentation and Measurement*, vol. 66, no. 1, pp. 131–140, 2016.

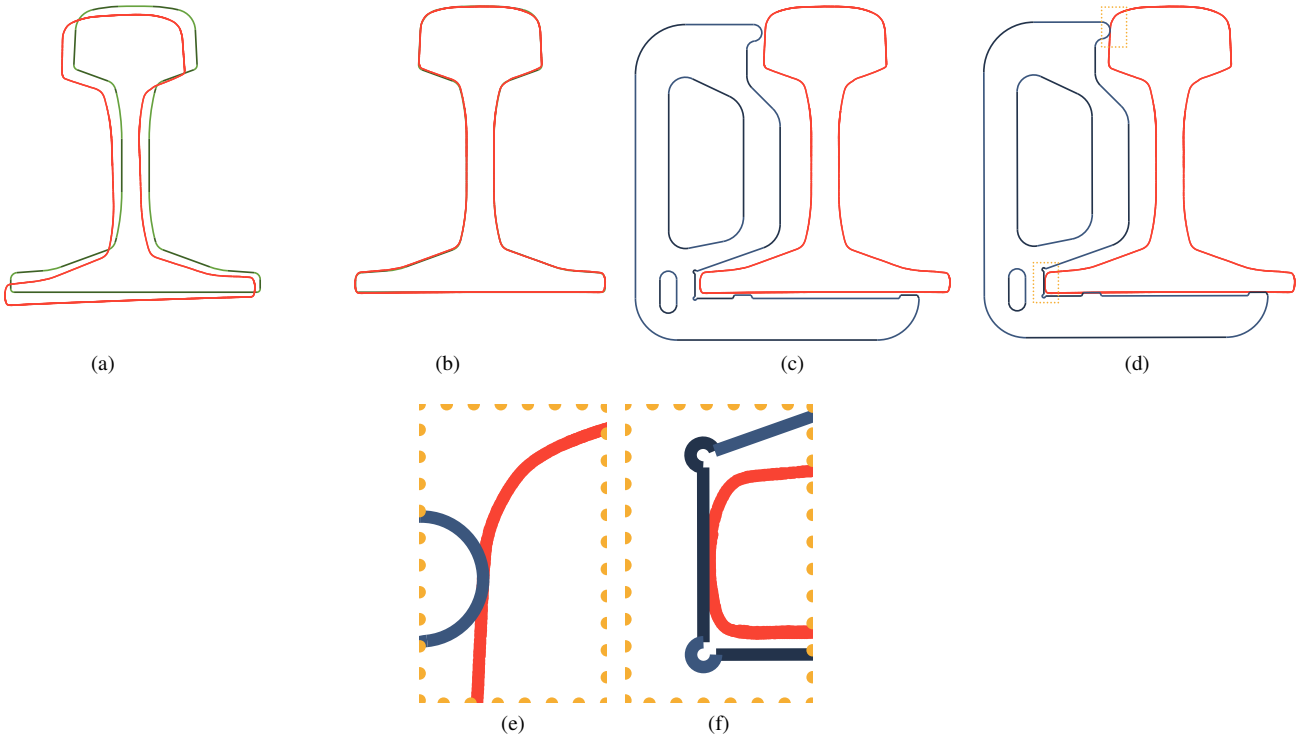

Fig. 9. Proposed approach applied to a real rail profile for testing the asymmetry. (a) Profile and model for the rail 60E1. (b) Alignment of the data with the model. (c) Course alignment of the data with the virtual gauge. (d) Fine alignment of the data with the virtual gauges. (e) Collision between the head of the rail and the virtual gauge. (f) Collision between the foot of the rail and the virtual gauge. This indicates a failed conformance test.

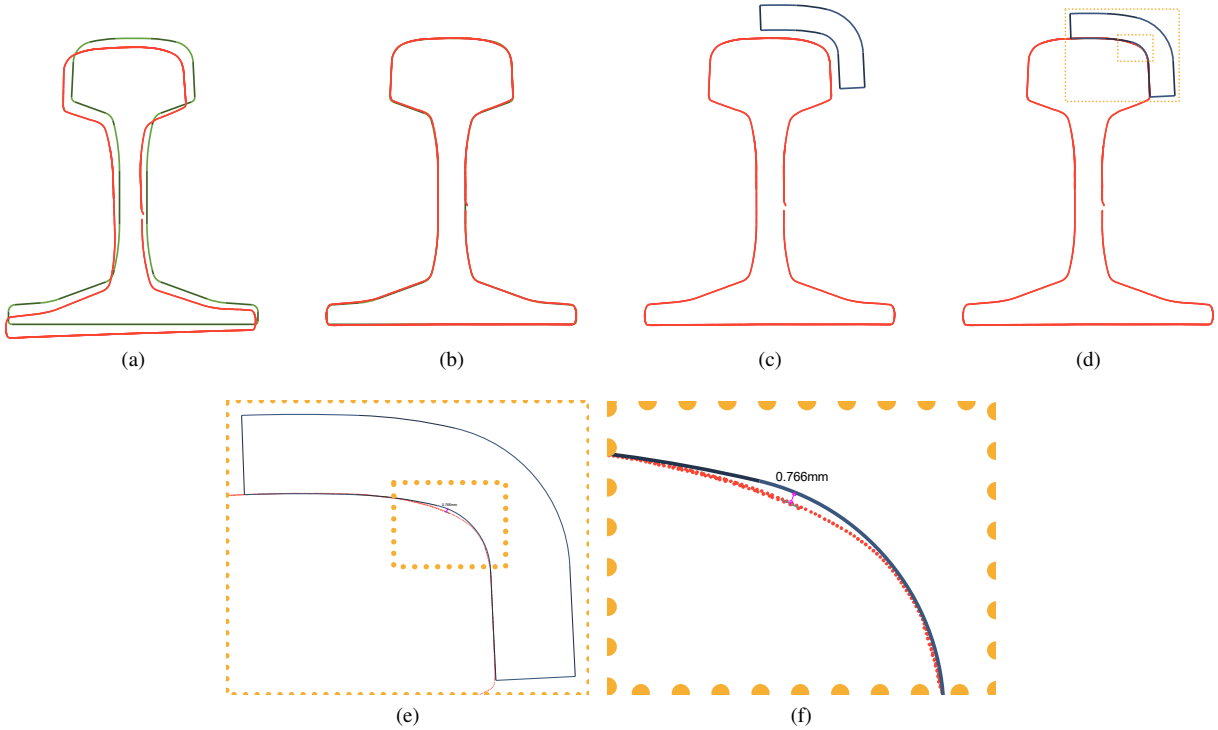

Fig. 10. Proposed approach applied to a real rail profile for testing the head. (a) Profile and model for rail 60E1. (b) Alignment of the data with the model. (c) Course alignment of the data with the virtual gauge. (d) Fine alignment of the data with the virtual gauges. (e) Enlarged area of the head. (f) Further enlarged area of the head showing a gap between the profile and the virtual gauge.

[8] D. Zhan, D. Jing, M. Wu, D. Zhang, L. Yu, and T. Chen, "An accurate and efficient vision measurement approach for railway catenary geometry parameters," *IEEE Transactions on Instrumentation and Measurement*, vol. 67, no. 12, pp. 2841–2853, 2018.

[9] Y. Li, X. Zhong, Z. Ma, and H. Liu, "The outlier and integrity detection of rail profile based on profile registration," *IEEE Transactions on Intelligent Transportation Systems*, 2019.

[10] E. C. for Standardization EN-13674-1, "Railway applications – track – rail – part 1: Vignole railway rails 46kg/m and above," 2011.

[11] P. Sroba and M. Roney, "Rail grinding best practices," in *Proceedings of AREMA Annual Conference, Chicago*, 2003.

[12] F. A. for Technical Regulation and Metrology, "Railway rails. general specifications," 2013.

[13] D. Flack, *Measurement Good Practice Guide No. 80*. Callipers and Micrometers. National Physical Laboratory, 2001.

[14] J.-C. Lombardo, M.-P. Cani, and F. Neyret, "Real-time collision detection for virtual surgery," in *Proceedings Computer Animation 1999*. IEEE, 1999, pp. 82–90.

[15] R. Usamentiaga, D. F. Garcia, and F. J. de la Calle Herrero, "Real-time inspection of long steel products using 3-d sensors: Calibration and registration," *IEEE Transactions on Industry Applications*, vol. 54, no. 3, pp. 2955–2963, 2018.

[16] S. Rusinkiewicz and M. Levoy, "Efficient variants of the icp algorithm," in *Proceedings Third International Conference on 3-D Digital Imaging and Modeling*. IEEE, 2001, pp. 145–152.

[17] D. W. Eggert, A. Lorusso, and R. B. Fisher, "Estimating 3-d rigid body transformations: a comparison of four major algorithms," *Machine vision and applications*, vol. 9, no. 5-6, pp. 272–290, 1997.

[18] A. Segal, D. Haehnel, and S. Thrun, "Generalized-icp." in *Robotics: science and systems*, vol. 2, no. 4. Seattle, WA, 2009, p. 435.